

Estimating Evaporation Fields and Specific Heats Through Atom Probe Tomography

Andrew P. Proudian¹ and Jeramy D. Zimmerman^{1, a)}
Colorado School of Mines

(Dated: August 6, 2020)

Estimations of evaporation field values in atom probe tomography (APT) literature are sparse despite their importance in the reconstruction and data analysis process. This work describes a straightforward method for estimating the zero-barrier evaporation field (F_E) that uses the measured voltage *vs.* laser pulse energy for a constant evaporation rate. This estimate depends on the sample radius of curvature and its specific heat (C_p). If a similar measurement is made of the measured voltage *vs.* base temperature for a fixed evaporation rate, direct extraction of the material's C_p can be made, leaving only the sample radius of curvature as an input parameter. The method is applied to extract F_E from a previously published voltage *vs.* laser pulse energy dataset for CdTe ($18.07 \pm 0.87 \text{ V nm}^{-1}$); furthermore, using the published voltage *vs.* base-temperature sweep of CdTe permits extraction of a specific heat ($11.27 \pm 2.54 \text{ J K}^{-1} \text{ mol}^{-1}$ at 23.1 K) in good agreement with the literature ($11.14 \text{ J K}^{-1} \text{ mol}^{-1}$ at 22.17 K). The method is then applied to the previously uncharacterized material tris[2-phenylpyridinato-C2,N]iridium(III) (Ir(ppy)₃), yielding $F_E = 7.49 \pm 0.96 \text{ V nm}^{-1}$ and $C_p = 173 \pm 27 \text{ J K}^{-1} \text{ mol}^{-1}$; this F_E is much lower than most materials characterized with APT to date.

As society demands ever more performant materials, detailed knowledge of nanostructure and composition becomes increasingly important. Unique among the many techniques for materials characterization, atom probe tomography (APT) combines high mass resolving power ($< 0.5 \text{ Da}$) and high spatial resolution ($< 1 \text{ nm}$) in the same analysis.¹

In APT, a sample is prepared with a small radius of curvature and a high bias is applied; this leads to a field at the surface of the sample of $> 1 \text{ V nm}^{-1}$. By applying an appropriate voltage or laser pulse, a single atom or molecule at the surface can be field ionized. The pulse-to-detection time and knowledge of the electric field allows the ion's mass-to-charge ratio and surface position to be determined. Repeating this process permits a three-dimensional, mass-specific reconstruction to be created.

When evaluating materials and understanding the evolution of an APT sample, it is important to know the evaporation field(s) of the surface atoms or molecules. This is useful both for the practical reason of improving the quality of reconstructions (*e.g.* through simulation), but also more broadly to clarify the physical process of field evaporation.^{2,3} Typical evaporation field values for elemental materials range from 20 to 150 V nm^{-1} ,^{4,5} but there are few tabulated values for more complex materials, with most being of solute atoms in a metallic matrix.^{4,6} As the APT community continues to expand the classes of materials it studies—such as ceramics, compound semiconductors, and organic small-molecules—the evaporation properties of these materials must be understood.^{1,7–9}

Due to the complexity of these new (for APT) material systems, a framework for experimentally determining the evaporation fields of materials is necessary, as computational methods struggle to work in these high-field

regimes (to say nothing of complex molecular systems).¹⁰ Furthermore, the experimental method must be fast and easy to perform so that it is adopted and evaporation field values become more regularly reported.

In this work, we propose a method to estimate the evaporation field based on a simple series of voltage *vs.* laser pulse energy measurements at a constant evaporation rate. These provide the necessary constraints on the governing equations to extract the zero-barrier evaporation field (F_E). We find that in a sample of CdTe for which data has been previously published our method extracts $F_E = 18.07 \pm 0.87 \text{ V nm}^{-1}$;¹¹ this agrees with F_E found on these data previously using the self-consistent reconstruction framework.¹² In addition, a measurement series of voltage *vs.* base temperature at a constant evaporation rate¹¹ recovers the specific heat (C_p) of the material ($C_p = 11.27 \pm 2.54 \text{ J K}^{-1} \text{ mol}^{-1}$) in good agreement with direct measurements.¹³

This method enables new measurements of F_E and C_p for the organic small-molecule tris[2-phenylpyridinato-C2,N]iridium(III) (Ir(ppy)₃), which has $F_E = 7.49 \pm 0.96 \text{ V nm}^{-1}$ and $C_p = 173 \pm 27 \text{ J K}^{-1} \text{ mol}^{-1}$.

To arrive at these estimates of F_E , we begin with the basic assumption that the field strength at the surface is given by¹⁰

$$F = \frac{V}{Rk_f},$$

where where all variable definitions are given in Table I. If the ionization process is thermally activated, the rate of ionization is¹⁰

$$r = An_{\text{hr}} \exp\left(-\frac{Q_n(F)}{k_B T}\right).$$

To estimate F_E , we assume ionization is a purely thermal process¹⁴ and that the function of the laser is to heat the tip. This assumptions allows us to change the

^{a)}Electronic mail: jdzimmer@mines.edu

denominator of the exponential as $k_B T \rightarrow k_B T + \alpha \delta E_p$. For the numerator of the exponential, close to F_E we can assume the field sensitivity is linear, taking the form $Q_n = \beta_n(F - F_E)$ because of the definition that $Q_n(F_E) \equiv 0$.^{10,15} With these simplifying assumptions, the rate equation becomes

$$r = An_{\text{hr}} \exp\left(-\beta_n \frac{\frac{V}{k_f R} - F_E}{k_B T + \alpha \delta E_p}\right).$$

Assuming a gaussian beam with a circular cross-section, this means that

$$\alpha(R) = 1 - \exp\left(-\frac{1}{2} \left(\frac{R}{\sigma}\right)^2\right).$$

With a sample detector distance of L and a detector radius for collected ions of r_d , we estimate the field of view assuming point projection from a spherical tip. The maximum angle is $\theta = \tan^{-1} \frac{r_d}{L}$, meaning that the visible area (A_s) is

$$A_s = 2\pi R^2 \frac{r_d/L}{\sqrt{1 + (r_d/L)^2}}.$$

Approximating an atom or molecule as having a circular cross-sectional area with radius d results in

$$n_{\text{hr}} = \eta \xi \frac{2(r_d/L)}{\sqrt{(r_d/L)^2 + 1}} \left(\frac{R}{d}\right)^2,$$

where η is the detection efficiency and ξ is the fraction of high probability surface molecules.

These simplifications result in the rate equation we will use to estimate F_E :

$$r = A\eta\xi \frac{2(r_d/L)}{\sqrt{(r_d/L)^2 + 1}} \times \left(\frac{R}{d}\right)^2 \exp\left(-\beta_n \frac{\frac{V}{k_f R} - F_E}{k_B T + \alpha \delta E_p}\right). \quad (1)$$

Using Equation 1, we know that for measurements on the same sample

$$\frac{V - V_E}{k_B T + \alpha \delta E_p} = \text{const.},$$

where we have converted $V_E = F_E k_f R$ because these are measured on the same sample and we assume the radius does not change over the course of the measurements (or can be corrected).¹¹ This means we can write

$$V = C\alpha\delta E_p + Ck_B T + V_E. \quad (2)$$

Thus, a fit to the form $ax + b$ on a measurement series of voltage *vs.* pulse energy allows us to extract $C = \frac{a}{\alpha\delta}$ and therefore

$$V_E = b - \frac{a}{\alpha\delta} k_B T.$$

Given the definition of δ in Equation 1, C_p of the material is given by

$$\delta = \frac{k_B}{C_p N_m},$$

where N_m is the number of moles of the material. Assuming both a spherical interaction volume of the laser with the sample that matches the sample radius of curvature R and a spherical atom or molecule with radius d , the measurements can be used to calculate C_p for the material under study:

$$\delta = \frac{k_B N_A d^3}{C_p R^3}. \quad (3)$$

This means that F_E becomes:

$$F_E = \frac{1}{k_f R} \left(b - \frac{a C_p R^3 T}{\alpha N_A d^3}\right). \quad (4)$$

The best way to estimate δ in Equation 2 is by measuring $V(T)$; that is, measure how voltage changes with temperature while holding the evaporation rate and pulse energy constant. We can calculate a value of δ by setting the two values of V_E equal, which is allowed because of the assumption of constant R :

$$\delta = \frac{b_T - b_E - \sqrt{(b_T - b_E)^2 + 4a_E a_T E_0 T_0}}{2a_T \alpha E_0 / k_B},$$

where the subscripts denote whether the coefficient is derived from the energy (E) or temperature (T) fit. Using Equation 3 this can be used to measure C_p for a material.

We test our method using CdTe, a well-characterized material. In 2015, Diercks and Gorman measured voltage *vs.* pulse energy and voltage *vs.* base temperature curves for CdTe, showing linear relationships in both series (see Figure 1) that are consistent with the above development.¹¹ For their data, the static radius assumption is fulfilled by the corrected voltage used to generate the curves, in which they accounted for the changing radius by correcting based on measured flux and transmission electron microscopy (TEM) measurements of the initial and final radius of the sample. This means that they set a reference tip shape and corrected subsequent datasets back to this shape; for the CdTe data, this is a radius of 140 nm.

Using the literature value of $C_p = 11.14 \text{ J K}^{-1} \text{ mol}^{-1}$ for CdTe at 22.17 K,¹³ the fit gives $F_E = 18.07 \pm 0.87 \text{ V nm}^{-1}$. This agrees with F_E previously reported for CdTe ($F_E = 12.4_{-4.3}^{+7.4} \text{ V nm}^{-1}$), but with significantly smaller uncertainty because we do not rely on the self-consistent reconstruction process and instead fit directly on the voltage *vs.* pulse energy series.¹² Fitting the voltage *vs.* base temperature curve using a value for d in Equation 3 of the distance between Cd and Te in a zinc blende crystal with a lattice constant of $a = 0.648 \text{ nm}$ gives $C_p = 11.27 \pm 2.54 \text{ J K}^{-1} \text{ mol}^{-1}$ for

| Variable | Description |
|----------|---|
| F_E | zero-barrier evaporation field |
| V | sample voltage |
| R | tip radius |
| k_f | field factor |
| k_B | Boltzmann constant |
| T | sample temperature |
| α | sample cross-section fraction |
| Q | field sensitivity |
| β | field sensitivity linear coefficient |
| δ | pulse energy conversion factor |
| L | sample-detector distance |
| r_d | detector radius |
| A_s | detector visible area |
| d | atomic/molecular radius |
| η | fraction of surface atoms/molecules likely to evaporate |
| ξ | detection efficiency |
| r | evaporation rate |
| E_p | laser pulse energy |
| C_p | specific heat |
| N_A | Avogadro's number |
| N_m | number of moles of the material |
| a_E | slope of the linear fit on pulse energy |
| a_T | slope of the linear fit on base temperature |
| b_E | intercept of the linear fit on pulse energy |
| b_T | intercept of the linear fit on base temperature |

Table I. The variables used for this development.

CdTe at 23.1 K, which compares quite favorably with the literature value.¹³ These two comparisons suggest that the assumptions of our development are reasonable and provide accurate estimates of F_E and C_p .

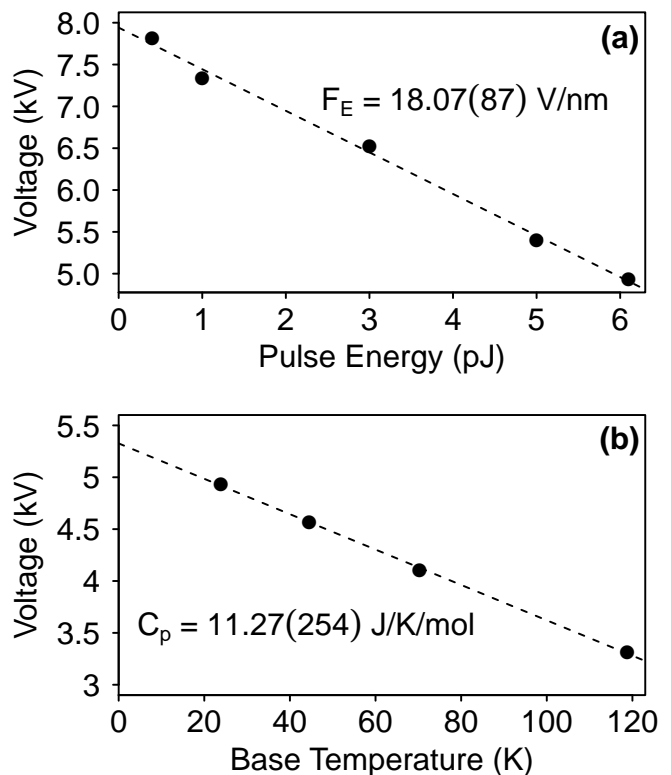
With these results obtained on CdTe matching the literature, it confirms our technique and permits us to move on to a new material. We fabricated a sample with a 102.4 nm thick film (measured by spectroscopic ellipsometry on a silicon witness) of Ir(ppy)₃ onto a silicon tip having a radius of $R = 256$ nm following the procedure outlined in Proudian *et al.*⁹ Each voltage measurement is the average voltage for evaporation of 5×10^4 ions at a fixed detection rate of 0.3%. The first 1.9×10^6 ions were omitted for sample alignment and radius equilibration.

The base temperature was set to 25, 45, and 35 K and then pulse energies were sequentially adjusted as 6, 12, 10, 8, 6, 4, 2, 1, and 6 pJ to generate the data shown in Figure 2. 4.9×10^6 ions were collected from the sample in total.

Fitting of this multivariate data to Equation 4 was performed using non-linear least-squares fitting *via* the `nls` function in the R package `stats`. The radius change of the sample is assumed to have the form

$$R = r_0 + r_f(1 - \exp(-N/n_r)), \quad (5)$$

where $r_0 = 256$ nm is the initial sample radius, r_f is the final sample radius increase, N is the number of evaporated ions, and n_r is an ion-radius constant. With this adjustment, the predicted voltage values based on this fit

Figure 1. (a) The univariate fit of voltage *vs.* pulse energy for the CdTe data in Diercks and Gorman.¹¹ (b) The univariate fit of voltage *vs.* base temperature for the CdTe data.

| Parameter | Value |
|-----------|---|
| F_E | $7.49 \pm 0.96 \text{ V nm}^{-1}$ |
| C_p | $173 \pm 27 \text{ J K}^{-1} \text{ mol}^{-1}$ |
| r_f | $114 \pm 49 \text{ nm}$ |
| n_r | $1.95 \pm 0.57 \times 10^6 \text{ Ion}$ |
| C | $1.510 \pm 0.094 \times 10^{12} \text{ V J}^{-1}$ |

Table II. The fitted values for the Ir(ppy)₃ data shown in Figure 2 based on a multivariate fit following Equation 2 using the radius assumption in Equation 5.

are shown in Figure 2; the values of the fitting parameters are given in Table II.

The linear behavior of both the CdTe and Ir(ppy)₃ samples suggests our thermal ionization assumption is valid for these materials. In contrast, the non-linear behavior of GaN observed by Diercks and Gorman suggests a different evaporation mechanism and hence is not amenable to this method of evaporation field extraction.¹¹

Applying APT to organic small-molecule semiconducting materials is just beginning, and there is much to learn about how these materials behave during field evaporation.⁷⁻⁹ The measured evaporation field of Ir(ppy)₃ is only $F_E = 7.49 \pm 0.96 \text{ V nm}^{-1}$, which is significantly lower than the fields typically measured for inorganic materials even though the mass of Ir(ppy)₃

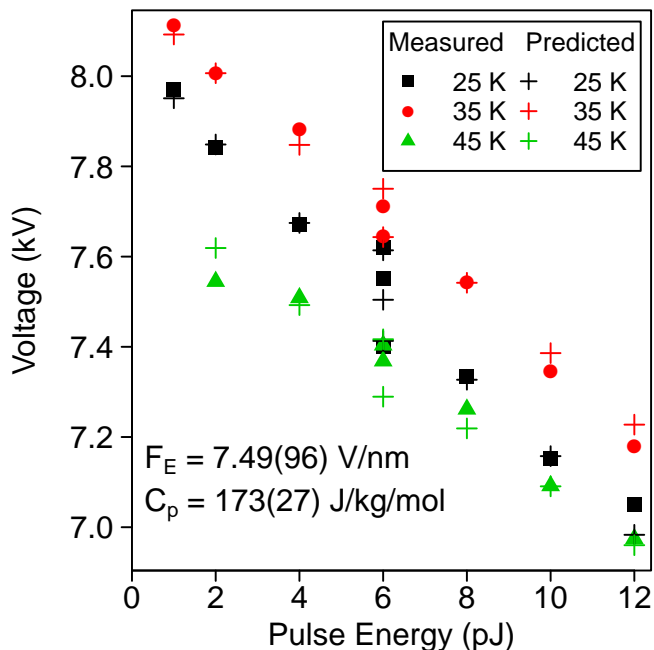


Figure 2. Equilibrium evaporation voltage of Ir(ppy)₃ vs. laser pulse energy, with different base temperatures shown in color. A multivariate fit following Equation 2 using the radius assumption in Equation 5 gives $F_E = 7.49 \pm 0.96 \text{ V nm}^{-1}$ and $C_p = 173 \pm 27 \text{ J K}^{-1} \text{ mol}^{-1}$, with other fitting parameters given in Table II; the predicted voltage values based on this fit are shown.

(654.78 Da) is much higher than the ions commonly observed in APT samples.^{4,5} This can be understood by considering that these solids are bound together by van der Waals bonds that are much weaker than the metallic or covalent bonds of the materials that are more commonly analyzed with APT.¹⁶ These weak van der Waals bonds have correspondingly low evaporation fields, which is why entire molecules in this class of materials can field evaporate without fragmenting when analyzed with APT.⁹

The inversion of the equilibrium voltage curves for the data at 25 and 35 K can be understood by recognizing the order in which these data were acquired and the consequent change in the sample radius of curvature ($R \approx 340$ to 348 nm at 25 K and $R \approx 357$ to 361 nm at 35 K); we accounted for this change using Equation 5 when estimating F_E and C_p .

Comparing the measured specific heat of $C_p = 173 \pm 27 \text{ J K}^{-1} \text{ mol}^{-1}$ for Ir(ppy)₃ with the measured value for C₆₀ at these temperatures of $C_p = 50 \text{ J K}^{-1} \text{ mol}^{-1}$ shows a comparable scale of C_p but higher, which is in line with the increased internal degrees of freedom for Ir(ppy)₃.¹⁷ This C_p appears constant over the range of temperatures measured (25 to 45 K); *i.e.*, adding in a linear slope correction to the fitting function results in a poorer quality model as tested using Schwarz’s Bayesian Criterion.¹⁸ This behavior is similar

to the relatively flat region of C_p for C₆₀ observed by Matsuo *et al.* in this temperature range.¹⁷

In conclusion, through APT measurements of voltage vs. laser pulse energy and voltage vs. temperature curves, estimates of the F_E can be achieved for materials where field evaporation is thermally activated. This method represents a simple way to estimate this quantity that has been under-reported in the literature. Using previously published data of CdTe,¹¹ we measure an evaporation field of $F_E = 18.07 \pm 0.87 \text{ V nm}^{-1}$, which matches a previously published value but with smaller error.¹² We also show that the assumptions permit recovery of the C_p of CdTe at 23.1 K of $C_p = 11.27 \pm 2.54 \text{ J K}^{-1} \text{ mol}^{-1}$. Comparing these values to the literature provides demonstrates that the method provides accurate estimates. The procedure is then applied to the organic small-molecule material Ir(ppy)₃, yielding $F_E = 7.49 \pm 0.96 \text{ V nm}^{-1}$ and $C_p = 173 \pm 27 \text{ J K}^{-1} \text{ mol}^{-1}$. This low F_E provides a starting point for understanding how small-molecule organic semiconducting materials behave in APT.

ACKNOWLEDGMENTS

This work was supported by the U.S. Department of Energy, Office of Science, Basic Energy Sciences under Award DE-SC0018021 and by funding from Universal Display Corporation. The Local Electrode Atom Probe™ 4000X Si (LEAP) was supported by a National Science Foundation Major Research Instrumentation grant DMR-1040456. Dr. David R. Diercks kindly provided the data for the CdTe analysis.¹¹

DATA AVAILABILITY STATEMENT

The data that support the findings of this study are available from the corresponding author upon reasonable request.

REFERENCES

- Y. Amouyal and G. Schmitz, MRS Bulletin **41**, 13 (2016).
- C. Oberdorfer, S. M. Eich, and G. Schmitz, Ultramicroscopy **128**, 55 (2013).
- F. Vurpillot, W. Lefebvre, J. M. Cairney, C. Oberdorfer, B. P. Geiser, and K. Rajan, MRS Bulletin **41**, 46 (2016).
- E. W. Müller and T. T. Tsong, *Field ion microscopy: principles and applications* (American Elsevier Publishing, New York, NY, 1969).
- B. Gault, M. P. Moody, J. M. Cairney, and S. P. Ringer, *Atom Probe Microscopy*, Springer Series in Materials Science, Vol. 160 (Springer New York, New York, NY, 2012).
- D. Brandon, Surface Science **5**, 137 (1966).
- D. Joester, A. Hillier, Y. Zhang, and T. J. Prosa, Microsc. Today **20**, 26 (2012).
- A. P. Proudian, M. B. Jaskot, C. Lyiza, D. R. Diercks, B. P. Gorman, and J. D. Zimmerman, Nano Letters **16**, 6086 (2016).

- ⁹A. P. Proudian, M. B. Jaskot, D. R. Diercks, B. P. Gorman, and J. D. Zimmerman, *Chemistry of Materials* **31**, 2241 (2019).
- ¹⁰D. J. Larson, T. J. Prosa, R. M. Ulfig, B. P. Geiser, and T. F. Kelly, *Local Electrode Atom Probe Tomography* (Springer New York, New York, NY, 2013).
- ¹¹D. R. Diercks and B. P. Gorman, *Journal of Physical Chemistry C* **119**, 20623 (2015).
- ¹²D. R. Diercks and B. P. Gorman, *Ultramicroscopy* **195**, 32 (2018).
- ¹³J. A. Birch, *Journal of Physics C: Solid State Physics* **8**, 2043 (1975).
- ¹⁴G. L. Kellogg, *Journal of Applied Physics* **52**, 5320 (1981).
- ¹⁵E. A. Marquis and F. Vurpillot, *Microscopy and Microanalysis* **14**, 561 (2008).
- ¹⁶J. S. Chickos and W. E. Acree, *Journal of Physical and Chemical Reference Data* **32**, 519 (2003).
- ¹⁷T. Matsuo, H. Suga, W. David, R. Ibberson, P. Bernier, A. Zahab, C. Fabre, A. Rassat, and A. Dworkin, *Solid State Communications* **83**, 711 (1992).
- ¹⁸Y. Sakamoto, M. Ishiguro, and G. Kitagawa, *Akaike Information Criterion Statistics* (Springer Netherlands, 1986).